Nano World Journal

http://dx.doi.org/10.17756/nwj.2017-038

Research Article

Open Access

Poly-lactic-co-glycolic acid Nanoformulation of Small Molecule Antagonist GANT61 for Cancer Annihilation by Modulating Hedgehog Pathway

Ankita Borah, Vivekanandan Palaninathan, Aswathy Ravindran Girija, Sivakumar Balasubramanian, Ankit K. Rochani, Toru Maekawa and D. Sakthi Kumar*

Bio-Nano Electronics Research Centre, Graduate School of Interdisciplinary New Science, Toyo University, Japan

***Correspondence to:**
Prof. D. Sakthi Kumar, PhD
Deputy Director, Bio-Nano Electronics Research Centre, Graduate School of Interdisciplinary New Science, Toyo University
Kawagoe Saitama, 350-8585, Japan
Tel: (+81)-(0) 492-39-1636/1375/1640
Fax: (+81)-(0) 366-77-1140
E-mail: sakthi@toyo.jp

Received: January 18, 2017
Accepted: January 31, 2017
Published: February 02, 2017

Citation: Borah A, Palaninathan V, Girija AR, Balasubramanian S, Rochani AK, et al. 2017. Poly-lactic-co-glycolic acid Nanoformulation of Small Molecule Antagonist GANT61 for Cancer Annihilation by Modulating Hedgehog Pathway. *NanoWorld J* 3(1): 1-10.

Published by United Scientific Group

Abstract

Targeting the self-renewal pathways (SRPs) in cancer has become one of the futuristic treatment strategies in order to prevent cancer relapse and drug resistance. One of the embryonic SRPs, Hedgehog (Hh) pathway is found to be aberrantly active in most of the cancers such as basal cell carcinoma, brain tumors, pancreas, prostate, leukemia's to name a few. GANT61, a hexahydropyrimidine derivative is a specific GLI1 inhibitor of the Hedgehog pathway known for its anticancer activity and also its ability to inhibit the self-renewal properties of cancer stem cells (CSCs). However, its clinical efficacy is limited due to its low water solubility, bioavailability and poor permeability. The objective of this paper is to present an effective nano drug delivery system for GANT61 to improve its water solubility, enhanced drug delivery with low toxicity to the healthy cells without compromising on the native behavior of the drug. We synthesized GANT61 PLGA nanoparticles through single emulsion solvent evaporation technique and studied the physicochemical properties of the nanoparticles. GANT61 PLGA NPs showed cytotoxicity against the cancer cells, with only minimal effect towards the normal cells. Furthermore, we also analyzed the inhibition of GLI1 nuclear translocation by GANT61 PLGA NPs using immunofluorescence staining. Our studies report the successful encapsulation of GANT61 inside polymeric nanoparticles with improved aqueous solubility, which resulted in cancer cells cytotoxicity and elimination of CSCs.

Keywords

Gli inhibitor, GANT61, GANT61 PLGA Nanoparticles, Single emulsion-solvent evaporation, Cancer therapy

Introduction

Cancer remains the leading cause of death worldwide surpassing that of heart disease with increasing numbers each passing year. The "classical hallmarks of cancer", which makes it a very complex disease includes invasion and metastasis, chronic proliferative signaling, activates angiogenesis, dodging the growth suppressors, resistance towards cell death and enabling replicative immortality [1]. Most of the cancers manifest these properties in the disease progression, however over the past decade many emerging hallmarks have been added to the list thus exhibiting another feature to the complexities of the disease. Advances in medical sciences though have been able to treat the deadly disease to a possible extent but a rise in cancer relapse and drug resistance have led to the failure of first line treatment strategies. In the last decade, prevailing theory of the existence

of a sub-population of cells in solid tumors known as cancer stem cells (CSCs); the "Achilles heel" of chemo-resistance and relapse have been reported [2, 3]. These CSCs are known to possess multi drug resistance pumps (MDR), self-renewal pathways (SRPs), specialized niche and altered metabolism. The presence of CSCs is reported in many devastating human malignancies such as acute myeloid leukemia [4], breast, brain [5], pancreas [6], prostate [7] to name a few. CSCs are known to be involved in metastasizing tumor, epithelial-mesenchymal transition (EMT) in addition to drug resistance and probable reason behind the failure of many oncologic therapies. It is imperative to design robust next generation therapeutics, to target the characteristic features of CSCs and prevent recurrence of the disease.

Taking into consideration of targeting the CSCs, the SRPs offer to be one of the cardinal targets in this direction. Hedgehog (Hh) signaling pathway, a prime SRP in maintaining the replicative potential of CSCs is involved in tumor growth, metastasis, and early and late mediator in human cancers [8]. The molecular pathogenesis of cancer in the context of Hh signaling arises through mutations in PTCH1, Smoothened (SMO), suppressor of fused (SUFU), and non-canonical activation of Gli transcription factors as well as autocrine and paracrine ligand dependent activation of the pathway. The association of dysregulated Hh signaling with cancer came from the studies of Hahn et al., where they found a rare condition of Gorlin syndrome, also known as basal cell carcinoma (BCC) [9]. BCC arises due to a mutation in PTCH1 and as a result of which it leads to a constitutive activation of the Hh pathway [9]. Apart from the activating mutations in the Hh pathway, tumors with over expressing ligands and aberrant activation of Hh target genes are also investigated in pancreatic, prostate, colon cancers among the few [10]. Hh signaling is also induced through crosstalk from other oncogenic pathways such as TGF-β, MAPK, PI3K pathways [11]. Experimental evidences represent Hh signaling as a potential target for the development of novel cancer therapeutics.

Pharmacological agents assigned to suppress Hh signaling in cancer comprises of naturally occurring compounds and small molecule antagonists such as, cyclopamine, resveratrol, GDC-0449 and IPI-926. All these Hh inhibitors designed are aimed at targeting the upstream component of the pathway such as PTCH, SMO mutations in cancer cells and fail to address the downstream scenario of the same. Non-canonical mode of Gli activation is implicated in many cancers, and hence needs to be addressed for effective cancer prevention. One of the second-generation inhibitors of Hh pathway is a small molecule antagonist called GANT61 discovered by Lauth et al., from a cell based screen for small molecule inhibitors [12]. GANT61 is proven to specifically inhibit Hh signaling by targeting the GLI 1/2 protein, which acts as a downstream component in the transcription of Hh targeted genes. GANT61 is also reported to be effective in tumors with PTCH or SMO mutations and eliminates CSCs to a significant level as compared to other Hh pathway antagonists such as cyclopamine and GDC- 0449 [13]. Several preclinical studies carried out in many cancer types both *in vitro* and *in vivo* have demonstrated the effectiveness of GANT61 in decreasing the target gene and protein expression of GLI1/2 and also PTCH1 [14]. GANT61 binds directly to GLI1 in close proximity independent of the DNA binding region of GLI1, thus showing its high specificity and minimizing off targets [15]. GANT61 also targets some of the "classical hallmarks of cancer" such as infinite replicative potential, apoptosis, DNA damage repair, EMT and autophagy, which supports the elimination of CSCs [16]. GANT61 was shown to effectively regress the pancreatic CSCs growth both *in vitro* and mice xenograft models, where the self-renewal capacity of the CSCs got compromised due to the blockade of Hh pathway [17]. Even though GANT61 exhibits high potency as an anticancer drug showing superior results both *in vitro* and *in vivo* conditions with a low cytotoxic dose between 5-20 μM, it encounters major limitation of aqueous solubility. Since free GANT61 is insoluble in media, it has to be solubilized in DMSO, which acts as a vehicle before administering to cell lines rendering a drawback for the drug for use in clinical translation [12, 17]. Therefore, delivery of GANT61 through novel drug delivery systems (NDDS), such as nanoparticles (NPs) is of vital interest in current cancer therapies, which also checks the corollaries of anticancer drug in the long run.

The formulation of anticancer drug into an appropriate drug delivery vehicle is of utmost importance, without generating any kind of immune response to other bodily compartments. The use of biodegradable and biocompatible polymers has been established to deliver many anticancer drugs successfully. Poly (lactic-co-glycolic acid) (PLGA) is a Food and Drug Administration (FDA) approved polymer that has been used for various biomedical applications including cancer drug delivery due to its attractive properties such as excellent biocompatibility, biodegradability, versatile release kinetics and ease of formulation methods adapted to hydrophobic, hydrophilic small molecules or macromolecules [18]. PLGA nano drug delivery systems ensure sustained release of drugs at their designated sites, while protecting the drug from degradation [18]. Easy surface functionalization of PLGA NPs helps in attaching several targeting moieties that provides an added advantage for a more targeted approach in cancer therapy.

The main objective of our work is to encapsulate GANT61 in PLGA NPs and to study their physicochemical properties in order to obtain a robust drug delivery system to target Hh signaling in various cancer cell lines without comprising the native nature and effectiveness of the drug. Biocompatible polymer based nanoparticles for cancer drug delivery will not only have improved water solubility and bioavailability but also have increased circulation time in bloodstream and active payloads in cancer cells [19]. The GANT61 PLGA NPs were synthesized using single emulsion solvent evaporation method and characterized to determine their size, surface morphology, and surface chemistry. Encapsulation efficiency and *in vitro* release kinetics were also investigated to check the efficacy of the prepared NPs as a coherent drug delivery system in cancer cell lines.

Experimental section

Materials

Poly (D, L-lactic-co-glycolic acid) (PLGA) (MW: 7,000-17,000, 50:50) and Polyvinyl alcohol (PVA), MW 31-50 kDa, 87-89% hydrolyzed, was procured from Sigma-Aldrich (St Louis, MO). The drug GANT61 was purchased from Abcam. Organic solvents such as ethyl acetate (EtAc), Dimethyl Sulfoxide (DMSO) and ethanol were purchased from Kanto chemicals, Japan. McCoy's 5A medium, Dulbecco's modified Eagle's medium (DMEM), Trypsin (0.25%), fetal bovine serum (FBS), penicillin (5000 U/ml)/streptomycin (5000 µg /ml) and Phosphate buffer saline (PBS) were procured from American Type Culture Collection (ATCC), USA and Gibco (Life Technologies) respectively. Alamar blue cell viability kit from Invitrogen, USA. Anti-Gli 1 antibody and Goat Anti-rabbit IgG H&L (Alexa Fluor 594) pre-adsorbed was purchased from Abcam. 16% Fomaldehyde, (Methanol free) and NucBlue Live Ready Probes Reagent was procured from ThermoFisher Scientific and Life Technologies respectively.

Preparation of GANT61 encapsulated PLGA nanoparticles

GANT61 loaded-PLGA nanoparticles were synthesized by single emulsion-solvent evaporation method, one of the widely-adopted methods to encapsulate hydrophobic compounds. In our study, we have referred to previously reported method for the preparation of PLGA nanoparticles [20]. Briefly, 20 mg of PLGA and 2 mg of GANT61 were dissolved in 2 ml of ethyl acetate and this mixture was left for complete dissolution for half an hour with intermittent vortexing. The PLGA-GANT61 mixture was added drop wise to 4 ml of 5% PVA aqueous solution under continuous magnetic stirring. PVA used acts as a surfactant for emulsification. This mixture was sonicated at 40 kHz for two minutes to create a fine emulsion and aids the formation of smaller polymeric droplets. The resulting emulsion was added to 100 ml of 0.3% PVA aqueous solution and stirred rapidly for five hours for ethyl acetate to evaporate. During the evaporation process the smaller polymeric droplets were hardened and collected by centrifugation process. Centrifuging the above mixture at 8,000 rpm for 30 minutes collected the GANT61 loaded-PLGA nanoparticles. The supernatant has been discarded and the pellet is washed thrice with ultra pure water. The synthesized nanoparticles were freeze dried and stored at -20 °C till further use. The drug free nanoparticles were also prepared by the same procedure.

Yield and encapsulation studies of GANT61 by UV-vis spectroscopy

The dry weight and yield of the nanoparticles was calculated using equation 1 [21].

$$\% \text{ Yield} = \frac{\text{Weight of nanoparticles obtained}}{(\text{Weight of GANT61+Weight of PLGA}) \text{ used for the nanoparticle synthesis}} \times 100 \quad ..(1)$$

Entrapment efficiency of GANT61 was calculated using the following equation 2 [21].

$$\% \text{ Encapsulation} = \frac{c_i - c_f}{c_i} \times 100 \quad .....(2)$$

Where, C_i is the initial drug concentration and C_f is the free drug concentration in the supernatant. A calibration curve of standard concentrations of GANT61 in ethanol (5-50 µg/ml) versus absorbance was measured by UV-vis spectrophotometer (DU730 Beckman Coulter) and plotted to determine the unknown quantity of free GANT61 present in the supernatant. The UV-Visible spectrum of GANT61 PLGA NPs was also recorded to check the presence of GANT61 and stability in the NPs. Briefly GANT61 PLGA NPs were suspended in ethanol and then centrifuged at 8000 rpm for 10 minutes. The supernatant was then subjected for wavelengths scan in the range 220-900 nm by using spectrophotometer.

Characterization of nanoparticles

GANT61 PLGA nanoparticles were dispersed in Milli Q water for performing all the analyses. The size and surface morphology of the prepared nanoparticles were characterized using scanning electron microscopy (SEM) JEOL (JSM-7400 F) and transmission electron microscopy (TEM) JEOL's JEM 2100 FS transmission electron microscope. For SEM studies 10 µL of water-dispersed nanoparticles were dropped onto a clean silicon (Si) wafer and vacuum dried. The dried sample was then subjected to sputter coated with platinum (Pt) for 40 seconds (Hitachi E-1030, Ion sputter). The Pt coated sample on Si substrate was then viewed under SEM operating at an accelerating voltage of 5 kV. For TEM imaging, a drop of sample was deposited on previously hydrophilized grid, air dried at room temperature and viewed under TEM.

Particle size distribution and the zeta-potential were measured using Zetasizer (Malvern, NanoZs). GANT61 PLGA NPs were suspended in Milli Q water and diluted prior to measurements. For particle size distribution analyses a disposable sizing cuvette was used and the mean diameter and polydispersity index (PDI) values were obtained at an scattering angle of 173 °C at 25 °C. Zeta potential measurements was carried out using a zeta dip cell also at 25 °C. In order to investigate the chemical bonding patterns and any other possible interaction between GANT61 and PLGA, ATR-Fourier Transform Infra-Red Spectroscopy (ATR-FTIR) (Thermo Scientific, Nicolet iS50 FT-IR) was performed with a resolution of 4 cm^{-1}, in the range of 4000 to 500 cm^{-1}.

Surface chemistry characterization

The surface chemistry of void PLGA NPs and GANT61 PLGA NPs was analyzed by X-ray photoelectron spectroscopy (XPS, AXIS His-165 Ultra, Kratos Analytical, Shimadzu Corporation, Japan). The binding energy spectra for all the samples were recorded from 0 to 1000 eV with 80 eV pass energy and dual Magnesium (Mg) as the transmission mode. Curve fitting analyses were carried out using the software provided by the manufacturer.

In vitro drug release studies

The *in vitro* drug release profile of GANT61 from GANT61 PLGA NPs was performed in PBS at different pH of 7.4 and 4.5. 2.5 mg of samples was dispersed in 5 ml each of PBS buffer and divided into 10 Eppendorf tubes with a

concentration of 250 µg/ 500 µl in each tube. All the tubes were maintained in a shaking incubator with a shaking speed of 120 rpm at 37 ˚C for 10 days. At predetermined time intervals the tubes were taken out and centrifuged at a speed of 15,000 rpm for 30 minutes. The supernatant was taken to measure the absorbance of the drug by UV-vis spectrophotometer. The release profile of GANT61 was calculated by the following equation 3 [22].

$$\% \text{ Release} = \frac{Release\ GANT61}{Total\ GANT61} \times 100 \quad \text{.....(3)}$$

Cell culture

Human colon cancer cell line (HT-29), breast cancer cell line (MCF-7) and mouse fibroblast-like cells (L929) were purchased from ATCC, USA and Riken Bio Resource Center, Japan. HT-29 cells were cultured in McCoy's 5A medium, and MCF-7 cells were cultured in DMEM, supplemented with 10% Fetal Bovine Serum (FBS), penicillin (5000 U/ml)/streptomycin (5000 µg /ml) at 37 ˚C in a humidified atmosphere of 5% CO_2 till 70-80% confluency is attained. The cells were sub cultured every 3 days and maintained in T25 flasks. L929 was also cultured in DMEM and used as a control cell line for the *in vitro* cytotoxicity studies.

In vitro cytotoxicity studies

The therapeutic efficacy and biocompatibility of GANT61 PLGA NPs on cancer cell and normal cells was evaluated by alamar blue colorimetric assay. The principle behind alamar blue assay is to monitor the reducing environment of the living cells where the main ingredient resazurin is reduced to highly fluorescent resorufin by metabolically active viable cells. The assay was performed as per the manufacturer's protocol.

For the assay, confluent cells were trypsinized, seeded in a microtiter 96-well plate at a density of 5-6 × 10^3 cells/ml and kept at 37 ˚C, 5% CO_2 for incubation. Following 24-hour incubation, medium was replaced with fresh media and GANT61 PLGA NPs in the concentration range of 50 µg/ml, 100 µg/ml, 250 µg/ml, 500 µg/ml and 1 mg/ml were added. The treated cells were then incubated for 24, 48 and 72 hours study period under same culture conditions. At the end of each incubation period, 10% of alamar blue dye was added to the cells, left for incubation for another 4 hours and fluorescence was recorded at 580-610 nm using a microplate reader (Power scan HT Microplate reader, Dainippon Sumitumo Pharma, Japan). The assay was carried out in three independent experiments all in triplicates and cell viability was calculated using the formula $\frac{A_{Test}}{A_{Control}} \times 100$, where Atest is the absorbance of the test sample and Acontrol is the absorbance of control sample. Untreated cells were taken as positive controls with 100% cell viability. Determination of cell viability in the presence of GANT61 PLGA NPs is an indirect measure of the cytotoxic effects of the NPs. The *in vitro* cytotoxicity of free GANT61 in 0.5% DMSO was also analyzed by alamar blue assay in the above cell lines. We also carried out optical microscopy to supplement the results of cytotoxic assay. The normal cells as well as the cancer cells were cultured in 6-well plates till confluent at a cell density of 10,000 cells/well. The cells were then treated with 1 mg/ml of GANT61 PLGA NPs for 3 days and then observed under LEICA DMi8 microscope.

Immunofluorescence staining

To examine the nuclear translocation of GLI1 after treatment with GANT61 PLGA NPs immunofluorescence staining was performed by formaldehyde-methanol fixation method. Cells were seeded at 4 × 10^4 cells/well until confluent in glass bottom dish. Cells were then treated with required concentration of NPs (1 mg/ml) and left for 24-hour incubation. After that cells were washed with PBS and fixed in 4% formaldehyde for 10-20 minutes. The cells were rinsed briefly with PBS and then permeabilized with cooled methanol for 5-10 minutes at -20 ˚C. After additional washings, cells were incubated with Gli1 polyclonal antibody overnight at 4 ˚C. Later the cells were labeled with goat antirabbit IgG Alexa Fluor-594 conjugated antibody for 30 minutes, then washed and incubated with NucBlue Live Ready Probes. The cells were observed and imaged under confocal laser scanning microscope (NIKON A1 plus).

Tumorsphere formation assay

The effect of GANT61 PLGA NPs on the CSC proportion of HT-29 and MCF-7 cells were determined by its ability to form tumorspheres *in vitro*. We carried out the tumorsphere assay as reported in [23] with slight modifications. Briefly HT-29 and MCF-7 cells were cultured in 12-well plates at a density of 5 × 10^4 cells per well till confluent. The cells were then treated with GANT61 PLGA NPs for 24 and 48-hours (1 mg/ml concentration) or left untreated. Following the treatment period the nanoparticles were removed and the cells were washed and incubated with fresh medium at 37 ˚C for 72 hours. Thereafter the cells were trypsinized and cultured in ultralow attachment 6-well dishes (Corning Incorporated, Corning, NY, USA) at a density of 2000 cells per well to obtain the tumorspheres. The cells were cultured in cancer stem cell conditioned medium (Cancer stem cell medium, Promocell). After 5-6 days the tumorspheres were observed under an optical microscope (LEICA DMi8 microscope). The tumorspheres are characterized by solid, round structures with cells fused together difficult to distinguish them as individual cells.

Results and Discussion

Synthesis and characterization of GANT61 loaded PLGA nanoparticles

To improve the aqueous solubility, bioavailability of GANT61, PLGA was used to synthesize the GANT61 PLGA nanoparticles and characterized for its morphology, size distribution and surface chemistry. We have used PLGA (50:50) owing to its unique degradation properties [24]. GANT61 PLGA NPs were synthesized by single emulsion-solvent evaporation method. The NPs were prepared in batches until the required amount of NPs needed for carrying out characterization and cell studies were achieved. Consistency

parameters were checked for different batches of NPs synthesized. Solvent evaporation method was found best suited method to synthesize NPs encapsulating hydrophobic drugs, as it increases the incorporation efficiency of drugs as well as the desired size of the NPs can be achieved by controlling the stirring rate and conditions [25, 26]. The prepared GANT61 PLGA NPs were completely soluble in water as compared to free GANT61, which is insoluble in water. The percentage yield for every batch of NPs synthesized was in the range of 25-27% and entrapment efficiency of 96-98%.

Under SEM observations as shown in Figure 1A and 1B, the synthesized GANT61 PLGA NPs had a varied size distribution from 200-400 nm and the morphology of the NPs was found to be spherical with a smooth surface. Similarly TEM image as shown in inset of Figure 1A also revealed NPs with a well-defined spherical shape. SEM and TEM analysis of the NPs also correlated with the dynamic light scattering (DLS) measurements. DLS measurements revealed nanoparticles with size distribution in the range of 150-450 nm and average hydrodynamic diameter of 250 nm (Supplementary Figure 1) and a polydispersity index (PDI) of 0.1-0.3. Surface charge of nanoparticles elucidates a significant influence on its cellular interaction and uptake. PLGA NPs tend to have a negative charge that can be brought to neutral or positive charge by appropriate surface modifications. Earlier reports suggest that the zeta potential of PLGA NPs is influenced by the end groups of PLGA, type of drug employed and the stabilizer used during preparation [27]. In this study GANT61 PLGA NPs had zeta potential in the range of -22 mV to -17 mV (Supplementary Figure 2). Zeta potential values also denote the colloidal stability of NPs, where highly charged particles tend to remain stable in colloidal suspensions. This could be attributed to the coulombic repulsion forces arising from their surface charge, which overcomes the van der Waals attractive forces between them [28]. It is quite evident from our zeta potential data that GANT61 PLGA NPs should be stored in lyophilized state and reconstituted just before administering rather than storing in liquid suspension to avoid stability issues [29].

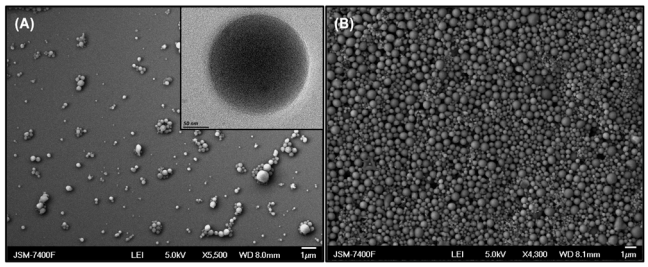

Figure 1: Electron microscopy studies. **(A & B)** SEM image of GANT61 PLGA NPs. (At scale 1μm). Inset of **1(A)** TEM image of GANT61 PLGA NPs. (At scale 50 nm).

FTIR analysis is a qualitative technique that measures the selective absorption of light by the vibration modes of specific chemical bonds in the sample. The observation of vibration spectrum of encapsulated drug allows evaluating the molecular interaction that might occur between the drug and polymer. Atomic vibrations involved in such interactions may have altered frequency and intensity [30, 31]. In the present work pure PLGA, pure GANT61 and GANT61 PLGA NPs were subjected to ATR-FTIR analysis and the spectra were obtained as shown in (Supplementary Figure 3). The ATR-FTIR analysis suggests that there was no chemical interaction between the drug and the polymer that could alter its chemical structure during the study.

Next, we determined the surface chemistry of the prepared NPs to check the presence of free drug on the surface of GANT61 PLGA NPs. GANT61 is the only component that contains nitrogen as observed in the XPS spectra of the free drug shown in Figure 2A. In the prepared NPs the presence of nitrogen peak can be a characteristic feature to determine the free drug on the surface of NPs. Wide scan of the GANT61 PLGA NPs (water treated) failed to detect the existence of N 1s signal on the surface of the NPs as shown in Figure 2A. Since GANT61 is a hydrophobic drug, its low solubility in water prevented its diffusion from the NPs and makes it to stay inside the polymeric NPs [32]. The absence of N 1s peak on the XPS spectra of GANT61 PLGA NPs clearly indicates the successful encapsulation of the drug inside the PLGA NPs or its negligible presence on the surface. For further confirmation, we dispersed the GANT61 PLGA NPs in ethanol and determined the XPS spectra for the presence of nitrogen, shown in Figure 2A. GANT61 has an affinity towards ethanol that allows the drug to diffuse out of the NPs and the same is confirmed by the presence of N 1s peak as recorded by the XPS spectra, thus confirming the encapsulation of GANT61. The XPS spectra of GANT61 PLGA NPs also clearly show the oxygen (O) 1s and carbon (C) 1s peak at 533 eV and 287 eV respectively confirming the oxygen and carbon elements of the PLGA polymer matrix, which is also present in the XPS spectra of the void PLGA NPs as shown in Figure 2A.

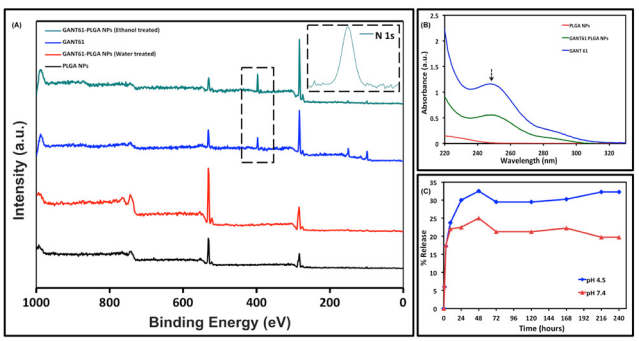

Figure 2: (A) XPS spectra of PLGA NPs, GANT61 PLGA NPs (water treated), GANT61, GANT61 PLGA NPs (ethanol treated). The presence of N1s peak in the spectra of GANT61 PLGA NPs (ethanol treated) indicates the encapsulation of GANT61 inside PLGA NPS. The peaks at 533 eV and 287 eV represent oxygen and carbon respectively. **(B)** UV-vis spectra of PLGA NPs, GANT61 PLGA NPs and GANT61. **(C)** *In vitro* drug release studies of GANT61 from GANT61 PLGA NPs at pH 4.5 & pH 7.4 PBS buffer.

The UV-vis spectra of GANT61, GANT61 PLGA NPs and PLGA NPs suspended in ethanol are depicted in Figure 2B. GANT61 (free drug) shows λ_{max} at two wavelengths, where a major peak was observed at 250 nm and a smaller shoulder peak was seen at 285 nm. A similar tendency was noted in the case of GANT61 PLGA NPs as well. Since GANT61 has a higher affinity towards ethanol, the drug diffuses out of

the GANT61 PLGA NPs and is completely miscible with it. However, the PLGA NPs did not show any λ_{max} as seen in the previous two spectra. This signifies the successful encapsulation of GANT61 in PLGA NPs, which is also supported by our XPS data.

In vitro drug release studies

The slow and controlled drug release from any versatile nanocarrier is a pre-requisite for successful biomedical applications with lesser side effects. *In vitro* release characteristics is influenced by a number of factors such as particle size, polymer degradation, and *in vitro* release medium [33]. In the present study the percentage release of GANT61 from GANT61 PLGA NPs under *in vitro* conditions at pH 7.4 and pH 4.5 is shown in Figure 2C. The release study of GANT61 PLGA NPs was investigated over a period of 10 days. We observed a slow and sustained release of GANT61 throughout the study period with maximum drug release of 32.5% at pH 4.5 after 48 hour, whereas at pH 7.4 there was only 25% of drug release after 48 hours. In both the pH conditions we could observe zero-order release of GANT61 after 48 hours independent of its concentration inside the PLGA NPs during the study period. An initial burst release of 17.5% was seen in the 3rd hour at both the pH conditions. Drug release from PLGA NPs mainly occurs by diffusion, polymeric erosion process or sometimes a combination of both [33]. Polymeric degradation also results from a number of factors such as change in pH, temperature and external stimuli, which accelerate drug release [34]. The release of GANT61 from the NPs was observed to be a pH dependent release profile resulting a slow drug release at physiological pH 7.4 and a faster release at acidic pH 4.5 corresponding to the acidic endosomal compartment after endocytosis. The difference in release rates at the different pH conditions could be due to two phenomena established from previous findings [27]. First, acidic condition accelerates the degradation of PLGA through bulk erosion [35]. This results in decreased molecular weight of the polymer and NPs mass loss, which leads to rapid dissolution of drugs in physiological fluids and subsequent release of the drug is enhanced. The second phenomenon that could be involved is accelerated polymer degradation and decreased ionic interaction between the drug and polymer at acidic pH. Betancourt et al., in their study observed a pH dependent release of doxorubicin (DOX) from doxorubicin loaded PLGA nanoparticles, which is related to the ionic interaction between the weakly basic DOX with the acid-capped PLGA, lactic acid and glycolic acid [27, 36]. Since drug release from PLGA nanoparticles can take from few days to months the release properties of GANT61 may be affected by the size, hardness and porosity of GANT61 PLGA NPs. Keum et al., reported the release of docetaxel PLGA NPs, where the release profile of docetaxel was not only influenced by different organic solvents but also different surfactants such as TPGS, poloxamer 188 and PVA while preparing the NPs [37]. Hence, the release of GANT61 can be controlled in the nanoformulated PLGA NPs thus, avoiding any toxic side effects.

In vitro cytotoxicity studies

The cytotoxic effect of free GANT61 has been studied earlier across various tumor cell lines [12, 17, 38] where GANT61 exhibited maximum toxicity within 48 hours. We studied the free drug cytotoxicity by using 0.5% DMSO as the solvent in a normal cell line L929, and two cancer cell lines HT-29, and MCF-7 using alamar blue assay. Choice of cancer cell lines was based on previous reports confirming the activity of free GANT61 against a human colon adenocarcinoma cell line and human breast cancer cell line [14, 39]. In both the cancer cell lines, we could observe immediate cell death within 24 hours even at the lowest concentration as shown in Figure 3C and 3E. The prolonged toxic effect of the drug is hindered due to its poor bioavailability, a desirable property for effective anticancer therapy. The cytotoxic effect of the drug is also seen in the L929 cell line after 48 hours at all the concentrations as shown in Figure 3A. These pitfalls could be overcome by a drug delivery protocol that could help maintain a therapeutic concentration of GANT61 for an extended period, to maximize its bioavailability, aqueous solubility for clinical efficacy, ensure sustained killing of cancer cells and sparing the normal cells.

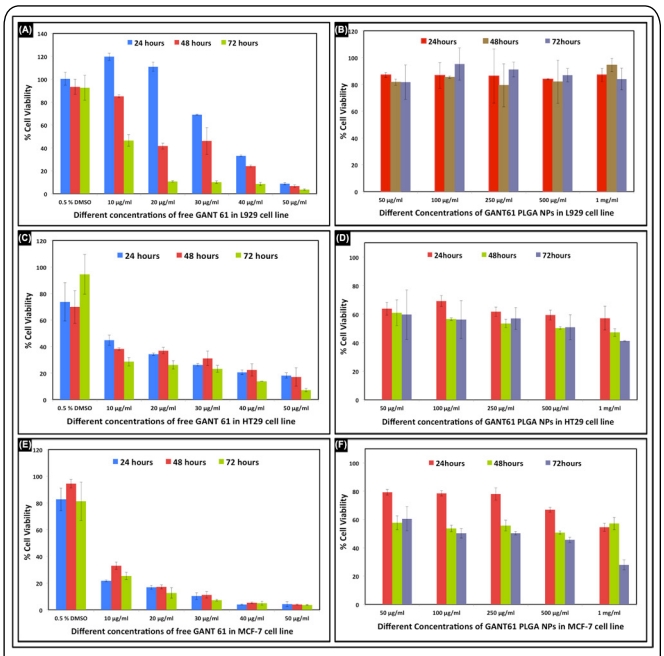

Figure 3: *In vitro* cytotoxicity assay on L929, HT-29, MCF-7 cells. **(A, C, E)** Free GANT61 cytotoxicity at 10 µg/ml, 20 µg/ml, 30 µg/ml, 40 µg/ml, and 50 µg/ml concentrations on L929, HT-29 and MCF-7 cells. 0.5% DMSO was used as a vehicle control. **(B, D, F)** GANT61 PLGA NPs cytotoxicity at 50 µg/ml, 100 µg/ml, 250 µg/ml, 500 µg/ml and 1 mg/ml concentrations on L929, HT- 29 and MCF-7 cells.

The cellular uptake of PLGA NPs is basically through endocytosis, where the rate and extent of the NPs uptake differs among cell lines. The biocompatibility of PLGA NPs as a nano carrier for anticancer drugs has been well studied in the past. Previous reports of using PLGA as nano carrier for encapsulating curcumin for anticancer therapy in eight different pancreatic cancer cell lines was demonstrated by Maitra et al. [40]. The void PLGA NPs used, as a control raised no toxicity in cell viability assays both *in vitro* and *in vivo*

across the cell lines. This illustrated excellent biocompatibility of PLGA NPs that can be used for the encapsulation of GANT61 as its nano vehicle. The therapeutic efficiency of GANT61 PLGA NPs was next determined on the same set of cell lines used earlier for free drug cytotoxicity by alamar blue assay. We carried out a dose and time dependent *in vitro* cell viability assay to assess the anticancer properties of GANT61 PLGA NPs at five different concentrations (50 µg/ml, 100 µg/ml, 250 µg/ml, 500 µg/ml, 1 mg/ml) for 24, 48 and 72 hours. L929, mouse fibroblast like cells did not show any cytotoxicity when treated with GANT61 PLGA NPs at all the mentioned concentrations till 72 hours, probably due to its low cellular uptake. L929 showed approximately 80-90% cell viability, even at higher dose of 1 mg/ml nanoformulation indicating the biocompatibility of the PLGA nanocarrier and also the non-toxic behavior of GANT61 towards normal cells as shown in Figure 3B. In the case of both the cancer cell lines HT-29 and MCF-7 we could observe reduced cell viability when treated with the drug nanoformulation. At a high dose of 1mg/ml of the drug nanoformulation both cancer cell lines HT-29 and MCF-7 exhibited around 54-57% cell viability after 24 hours. This could be due to the fact that low cellular uptake of NPs and a significant amount of GANT61 may not be released to mediate cytotoxicity. After 48 and 72 hours we could observe much reduced cell viability in both the cancer cell lines. Since the toxic effect of GANT61 is dose and time dependent, hence a prolonged incubation time with the NPs might have resulted in effective toxicity towards the cancer cell lines after 48 hours at all concentrations. This correlates with the *in vitro* release profile where maximum drug is released after 48 hours at pH 4.5. HT-29 was seen to exhibit 41.23% cell viability when treated with 1 mg/ml of drug nanoformulation after 72 hours and more or less same percentage of reduced cell viability at the other concentrations as shown in Figure 3D. As depicted in Figure 3F MCF-7 showed reduced cell viability of 27.94% when treated with 1 mg/ml dose of drug nanoformulation. This could be attributed to the release of an appropriate therapeutic concentration of drug from the GANT61 PLGA NPs that render sustained cytotoxicity towards the cancer cells with extended periods of incubation time. Two distinct but not exclusive theories provides justification for enhanced cytotoxic activity of anti-tumoral drugs encapsulated inside NPs from earlier findings. (i) NPs tend to adsorb onto the cellular membrane, leading to increased drug concentration near the cell surface. This creates a concentration gradient that would favor drug influx into the cell [41]. (ii) Secondly tumor cells are known to exhibit enhanced endocytic activity as a result of which polymeric nanoparticles are readily internalized. This activity allows the release of drugs into the interior of cells, thus contributes to increased drug concentration near the site of action [42]. In comparison to L929, both the cancer cell lines were seen to exhibit better cytotoxic effect when treated with GANT61 PLGA NPs demonstrating the specificity of the drug in killing the cancer cells while sparing the normal cells.

From the cytotoxicity assay, we inferred that GANT61 PLGA NPs induced maximum toxicity to the cancer cells at 1 mg/ml concentration. We further performed optical microscopy to explore the effects of nanoformulation on the normal and cancer cell lines. The cells were cultured in 6-well plates and treated with 1mg/ml of GANT61 PLGA NPs for 3 days. After the third day of treatment the particles were removed, replaced with fresh media and observed under Leica DMi8 microscope. As observed in Figure 4A the control L929 cells appeared to be spindle-shaped and adhered to the culture plate. The treated L929 cells showed minimal mortality and maintained its morphology as shown in Figure 4B. Control HT-29 cells are morphologically undifferentiated and grow as a multilayer of unpolarized cells when confluent [43] as shown in Figure 4C. HT-29 cells when treated with GANT61 PLGA NPs showed shrunken cell morphology, presence of cellular debris and rounded up cells, which has detached from the culture plate in comparison to the control cells as shown in Figure 4D. Breast cancer cells falls into four classes of morphologies when cultured in two and three dimensions namely round, mass, grape-like and stellate [44]. MCF-7 cells belong to the class of mass morphology characterized by colony formation, disorganized nuclei and filled colony centers [44]. A similar phenotype was observed in the control MCF-7 cells shown in Figure 4E. However when the MCF-7 was subjected to GANT61 PLGA NPs treatment, loss of colony formation ability and membrane blebbing was seen, in contrast to the control cells as observed in Figure 4F. The phase contrast images were a supporting evidence for the cytotoxic results and these finding clearly suggests that our GANT61 PLGA NPs were successful in imparting anti-cancerous activity without compromising the native behavior of the drug.

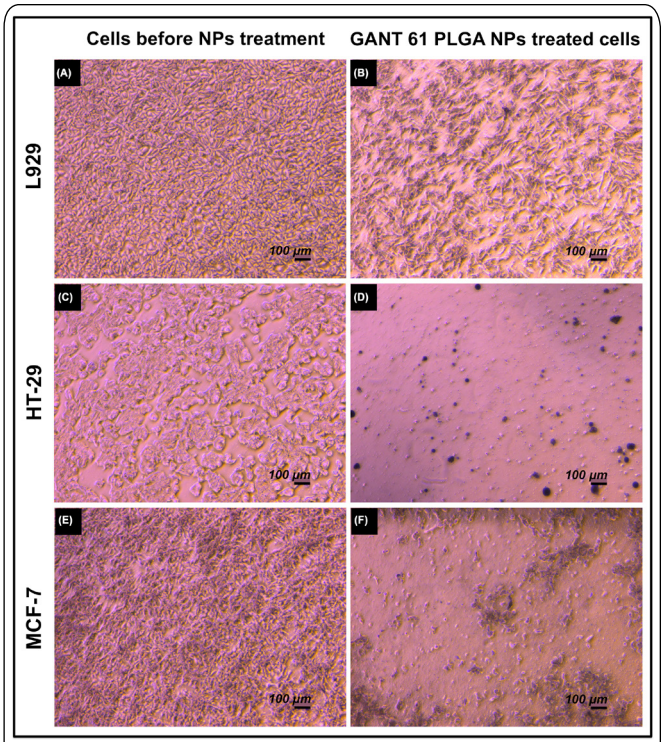

Figure 4: Therapeutic potential of GANT61 PLGA NPs in L929, HT-29 and MCF-7 cells. **(A)** L929 cells before NPs treatment. **(B)** L929 cells after treatment with GANT61 PLGA NPs. **(C)** HT-29 cells before NPs treatment. **(D)** HT-29 cells seen to be affected by the presence of GANT61 PLGA NPs with shrunken cell morphology. **(E)** MCF-7 cells before NPs treatment. **(F)** MCF-7 cells seen to have reduced colony formation after GANT61 PLGA NPs treatment (At scale 100 µm).

Immunofluorescence staining

GLI1 over expression is one of the factors resulting in the aberrant signaling of Hh pathway in many cancers. The activation of GLI1 promotes its translocation to the nucleus resulting in the initiation of transcription of Hh targeted genes. GANT61 is a potent inhibitor of GLI1 transcription factor inhibiting the Hh-Gli dependent cell survival [45]. GANT61 inhibits the downstream Hh signaling by blocking the nuclear translocation of GLI1 and prevents it from activating the Hh targeted genes. This blockade of GLI1 nuclear translocation also leads to its reduced expression in the nucleus, which can be qualitatively confirmed by immunofluorescence analysis. Both HT-29 and MCF-7 cells when treated with the appropriate concentration (1 mg/ml) of GANT61 PLGA NPs for 24-hours we can observe the inhibition of GLI1 nuclear translocation based on fluorescence intensity of GLI1 from the immunofluorescence analysis as shown in Figure 5 and 6 respectively. Hoechst stain is a nucleic acid stain that emits blue fluorescence when bound to DNA. GANT61 PLGA NPs targets GLI1 through passive drug targeting, which clearly relies on the "Enhanced Permeability and Retention" effect (EPR) and requires prolonged circulation of nanocarrier for better efficacy of the drug. Since the cancer cells were subjected to GANT61 PLGA NPs treatment for a period of 24-hours, it might not have resulted in a significant reduction of GLI1 expression owing to the passive mode of NPs uptake, which also correlates with the 24-hour cytotoxicity results. The fluorescence intensities of GLI1 in the nucleus of HT-29 and MCF-7 cells somewhat reduced in comparison to the control cells, which might suggest that GANT61 PLGA NPs were successful in inhibiting GLI1 nuclear translocation. L929 cells were also treated with 1 mg/ml of GANT61 PLGA NPs for 24-hours and subjected to immunofluorescence analysis. The fluorescence intensities were retained in the cytoplasm and nucleus both in control and treated cells as shown in (Supplementary Figure 4). This clearly suggests that the L929 cells exhibited low cellular uptake of NPs, hence resulted in lesser inhibition of GLI1 compared to the cancer cells. Recent study on the inhibition of GLI1 nuclear translocation after GANT61 treatment was carried out by Benvenuto et al., in breast cancer cell lines where decreased nuclear GLI1 expression in MCF-7 and SKBR-3 cell line was observed from the immunofluorescence analysis [39]. These findings suggest that GANT61 PLGA NPs are effective in blocking the Hh pathway by curbing the GLI1 nuclear translocation.

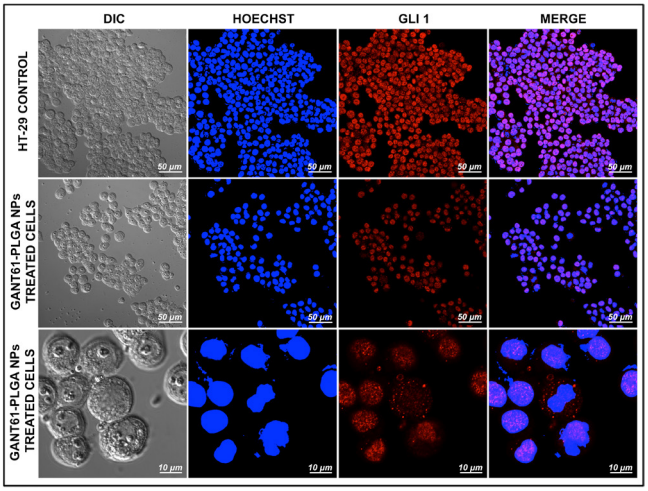

Figure 5: Confocal laser scanning microscopy. Immunofluorescence staining on HT-29 cells to check inhibition of GLI1 nuclear translocation. HT-29 cells are treated with GANT61 PLGA NPs for 24 hours. The top panel shows the control HT-29 cells (At scale 50 µm). The second panel shows the HT-29 cells treated with GANT61 PLGA NPs (At scale 50 µm). The third panel shows a magnified section of cells of the second panel (At scale 10 µm).

Tumorsphere formation assay

CSCs are pluripotent and progenitor cells having the ability to form new tumor masses even after therapeutic intervention owing to their self-renewal properties. The self-renewal ability of CSCs is constantly expanding that subsequently expands the tumor due to disruptions of genes involved in the regulation of self-renewal pathways [46]. Some of the genes involved in tight regulation of self-renewal pathways in normal stem cells are also implicated to be deregulated in the CSCs consequently giving rise relapse and drug resistivity. These pathways include the Hedgehog, Notch, WNT and BMI-1 demonstrated to play a pivotal role in malignant transformation [46]. Hence targeting of these pathways in CSCs provides a rationale for exploring novel clinical strategies to prevent permanent remission or even cure. The ability of CSCs to form tumorspheres can be assessed by the tumorsphere assay in *in vitro* conditions that can initiate and maintain tumors in the absence of cellular interaction and adhesion, when cells are grown under low-attachment conditions with minimal growth factor supplementation [47].

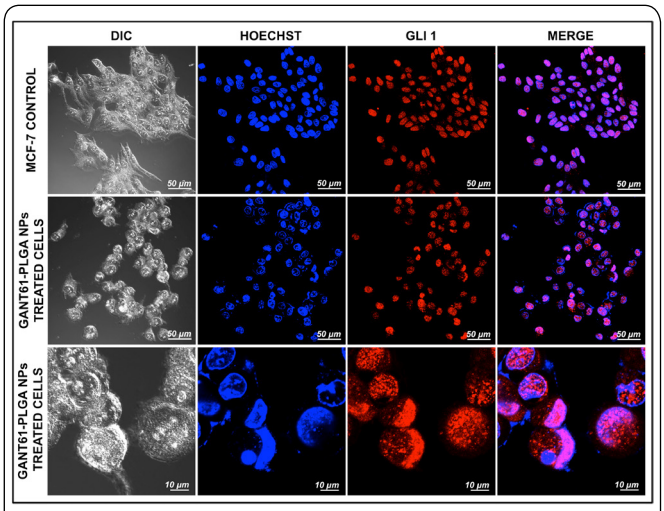

Figure 6: Confocal laser scanning microscopy. Immunofluorescence staining on MCF-7 cells to check inhibition of GLI1 nuclear translocation. MCF-7 cells are treated with GANT61 PLGA NPs for 24 hours. The top panel shows the control MCF-7 cells (At scale 50 µm). The second panel shows the MCF-7 cells treated with GANT61 PLGA NPs (At scale 50 µm). The third panel shows a magnified section of cells of the second panel (At scale 10 µm).

We performed a qualitative time dependent tumorsphere assay to evaluate the effect of GANT61 PLGA NPs on the CSC proportion of HT-29 and MCF-7 cell lines. Both of these cancer cell lines are known to form tumors in suspension culture when grown under cancer stem cell medium. HT-29 and MCF-7 were treated with the appropriate concentration of GANT61 PLGA NPs (1 mg/ml) for 24 and 48 hours.

Following the treatment when the cells were allowed to grow under stem cell conditions for a week to evaluate the formation of tumorspheres, it was observed that the ability to form tumorspheres was much reduced in the treated cells in comparison to the control cells as shown in Figure 7. This could be attributed due to the blockade of Hh pathway by GANT61 PLGA NPs, which resulted in the inhibition of self-renewing capacity. The control cells were seen to form tumorspheres in large numbers where cells fused together and were difficult to distinguish the individual cells (Figure 7A and 7D). Both HT-29 and MCF-7 when subjected to a 24-hour GANT61 PLGA NPs treatment, the cells were still able to form tumorspheres as shown in Figure 7B and 7E. This could be due to the low cytotoxicity imparted by the NPs that have sustained the self-renewing capacity of the cells to form tumorspheres. Whereas when the cells were treated with the NPs for 48-hours it was observed that the tumor forming capacity greatly reduced (Figure 7C and 7F). Aggregated and single cells were only observed in both the cell lines. The tumorsphere assay clearly suggests that GANT61 PLGA NPs were successful in inhibiting the Hh pathway and not only compromised the self-renewal but also the proportion of CSCs in HT-29 and MCF-7 cells.

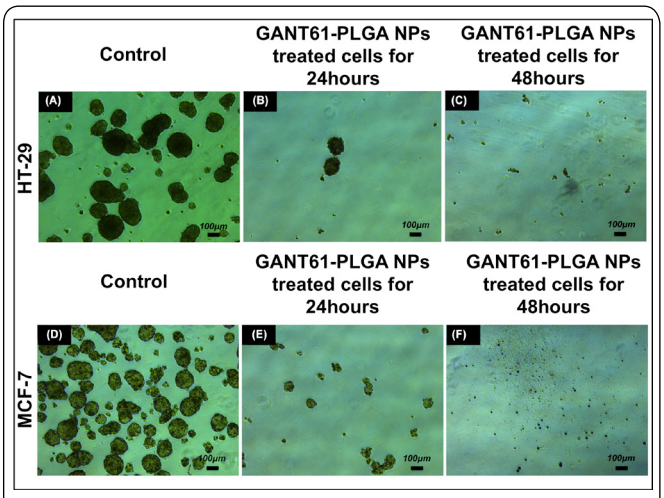

Figure 7: Tumorsphere formation ability of CSCs in HT-29 and MCF-7 cells. **(A)** HT-29 cells before NPs treatment. **(B & C)** HT-29 cells treated with GANT61 PLGA NPs for 24 hours and 48 hours and then grown in stem cell culture conditions, showing reduced tumorsphere formation in comparison to control cells (At Scale 100 µm). **(D)** MCF-7 cells before NPs treatment. **(E & F)** MCF-7 cells treated with GANT61 PLGA NPs for 24 and 48 hours, shows reduced mammosphere formation in *in vitro* stem cell conditions (At Scale 100 µm).

Conclusion

Present study reports the nanoformulation of GANT61 PLGA NPS. Encapsulation of GANT61 into PLGA NPs rendered improved aqueous solubility, bioavailability, controlled release and protection to the drug while also contributing to the maintenance of its activity. We determined the λMAX and drug entrapment efficiency of GANT61 through UV-vis spectroscopy. The results revealed high entrapment efficiencies of GANT61 in the PLGA NPs. The average size of GANT61 PLGA NPs was ~250 nm. *In vitro* release studies demonstrated the sustained release of GANT61 from the PLGA NPs as a result of which increased concentration of drug can be achieved near the site of action. The GANT61 PLGA NPs were shown to have efficient anti-tumor efficacies towards cancer cells while posing no toxic effects to the normal cells. Since GANT61 is a GLI1 inhibitor, immunofluorescence analysis also demonstrated that GANT61 PLGA NPs was able to block the nuclear translocation of GLI1 in the cancer cells. The tumorsphere formation assay, which is an index of self-renewal capacity of CSCs *in vitro*, further, confirmed the ability of GANT61 PLGA NPs to reduce the proportion of CSCs in the cancer cell lines. These findings reveal an effective *in vitro* GANT61 PLGA nanoformulation that holds a great prospect for future cancer therapy.

Acknowledgements

Ankita Borah and Ankit Rochani would like to acknowledge their sincere gratitude to the Ministry of Education, Culture, Sports, Science and Technology (MEXT), Japan for the financial support under the Monbukagakusho fellowship during the research. We would also like to express our sincere gratitude for Inoue Enryo Research Grant and program of the strategic research foundation for private universities S1101017, organized by MEXT, Japan since 2012 for providing additional financial support for this work.

References

1. Hanahan D, Weinberg RA. 2011. Hallmarks of cancer: the next generation. *Cell* 144(5): 646-674. doi: 10.1016/j.cell.2011.02.013
2. Liu G, Yuan X, Zeng Z, Tunici P, Ng H, et al. 2006. Analysis of gene expression and chemoresistance of CD133+ cancer stem cells in glioblastoma. *Mol Cancer* 5: 67. doi: 10.1186/1476-4598-5-67
3. Singh A, Settleman J. 2010. EMT, cancer stem cells and drug resistance: an emerging axis of evil in the war on cancer. *Oncogene* 29(34): 4741-4751. doi: 10.1038/onc.2010.215
4. Bonnet D, Dick JE. 1997. Human acute myeloid leukemia is organized as a hierarchy that originates from a primitive hematopoietic cell. *Nat Med* 3(7): 730-737. doi: 10.1038/nm0797-730
5. Singh SK, Clarke ID, Terasaki M, Bonn VE, Hawkins C, et al. 2003. Identification of a cancer stem cell in human brain tumors. *Cancer Res* 63(18): 5821-5828. doi: 10.1038/nature03128
6. Li C, Heidt DG, Dalerba P, Burant CF, Zhang L, et al. 2007. Identification of pancreatic cancer stem cells. *Cancer Res* 67(3): 1030-1037. doi: 10.1158/0008-5472.CAN-06-2030
7. Collins AT, Berry PA, Hyde C, Stower MJ, Maitland NJ. 2005. Prospective identification of tumorigenic prostate cancer stem cells. *Cancer Res* 65(23): 10946-10951. doi: 10.1158/0008-5472.CAN-05-2018
8. Thayer SP, di Magliano MP, Heiser PW, Nielsen CM, Roberts DJ, et al. 2003. Hedgehog is an early and late mediator of pancreatic cancer tumorigenesis. *Nature* 425(6960): 851-856. doi: 10.1038/nature02009
9. Hahn H, Wicking C, Zaphiropoulous PG, Gailani MR, Shanley S, et al. 1996. Mutations of the human homolog of Drosophila patched in the nevoid basal cell carcinoma syndrome. *Cell* 85: 841-851. doi: 10.1016/S0092-8674(00)81268-4
10. Rimkus TK, Carpenter RL, Qasem S, Chan M, Lo HW. 2016. Targeting the sonic hedgehog signaling pathway: review of smoothened and GLI inhibitors. *Cancers (Basel)* 8(2): 22. doi: 10.3390/cancers8020022
11. Lauth M, Toftgård R. 2007. Non-canonical activation of GLI transcription factors: implications for targeted anti-cancer therapy. *Cell Cycle* 6(20): 2458-2463. doi: 10.4161/cc.6.20.4808
12. Lauth M, Bergström Å. 2007. Inhibition of GLI-mediated transcription and tumor cell growth by small-molecule antagonists. *Proc Natl Acad Sci*

U S A 104(20): 8455-8460. doi: 10.1073/pnas.0609699104

13. Huang L, Walter V, Hayes DN, Onaitis M. 2014. Hedgehog-GLI signaling inhibition suppresses tumor growth in squamous lung cancer. *Clin Cancer Res* 20(6): 1566-1575. doi: 10.1158/1078-0432.CCR-13-2195
14. Mazumdar T, DeVecchio J, Shi T, Jones J, Agyeman A, et al. 2011. Hedgehog signaling drives cellular survival in human colon carcinoma cells. *Cancer Res* 71(3): 1092-1102. doi: 10.1158/0008-5472.CAN-10-2315
15. Agyeman A, Jha BK, Mazumdar T, Houghton JA. 2014. Mode and specificity of binding of the small molecule GANT61 to GLI determines inhibition of GLI-DNA binding. *Oncotarget* 5(12): 4492-4503. doi: 10.18632/oncotarget.2046
16. Gonnissen A, Isebaert S, Haustermans K. 2015. Targeting the Hedgehog signaling pathway in cancer: beyond smoothened. *Oncotarget* 6(16): 13899-13913. doi: 10.18632/oncotarget.4224
17. Fu J, Rodova M, Roy SK, Sharma J, Singh KP, et al. 2013. GANT-61 inhibits pancreatic cancer stem cell growth *in vitro* and in NOD/SCID/IL2R gamma null mice xenograft. *Cancer Lett* 330(1): 22-32. doi: 10.1016/j.canlet.2012.11.018
18. Danhier F, Ansorena E, Silva JM, Coco R, Le Breton A, et al. 2012. PLGA-based nanoparticles: An overview of biomedical applications. *J Control Release* 161(2): 505-522. doi: 10.1016/j.jconrel.2012.01.043
19. Cho K, Wang X, Nie S, Chen Z, Shin DM. 2008. Therapeutic nanoparticles for drug delivery in cancer. *Clin Cancer Res* 14(5): 1310-1316. doi: 10.1158/1078-0432.CCR-07-1441
20. Mathew A, Fukuda T, Nagaoka Y, Hasumura T, Morimoto H, et al. 2012. Curcumin loaded-PLGA nanoparticles conjugated with Tet-1 peptide for potential use in Alzheimer's disease. *PLoS One* 7(3): e32616. doi: 10.1371/journal.pone.0032616
21. Mukerjee A, Vishwanatha JK. 2009. Formulation, characterization and evaluation of curcumin- loaded PLGA nanospheres for cancer therapy. *Anticancer Res* 29(10): 3867-3875.
22. Sivakumar B, Aswathy RG, Nagaoka Y, Iwai S, Venugopal K, et al. 2013. Aptamer conjugated theragnostic multifunctional magnetic nanoparticles as a nanoplatform for pancreatic cancer therapy. *RSC Adv* 3(43): 20579-20598. doi: 10.1039/c3ra42645a
23. Ni MZ, Xiong M, Zhang XC, Cai GP, Chen HW, et al. 2015. Poly(lactic-co-glycolic acid) nanoparticles conjugated with CD133 aptamers for targeted salinomycin delivery to $CD133^+$ osteosarcoma cancer stem cells. *Int J Nanomedicine* 10(1): 2537-2554. doi: 10.2147/IJN.S78498
24. Makadia HK, Siegel SJ. 2011. Poly lactic-co-glycolic acid (PLGA) as biodegradable controlled drug delivery carrier. *Polymers (Basel)* 3(3): 1377-1397. doi: 10.3390/polym3031377
25. Mainardes RM, Evangelista RC. 2005. PLGA nanoparticles containing praziquantel: effect of formulation variables on size distribution. *Int J Pharm* 290(1-2): 137-144. doi: 10.1016/j.ijpharm.2004.11.027
26. Mu L, Feng SS. 2003. A novel controlled release formulation for the anticancer drug paclitaxel (Taxol): PLGA nanoparticles containing vitamin E TPGS. *J Control Release* 86(1): 33-48. doi: 10.1016/S0168-3659(02)00320-6
27. Betancourt T, Brown B, Brannon-Peppas L. 2007. Doxorubicin-loaded PLGA nanoparticles by nanoprecipitation: preparation, characterization and *in vitro* evaluation. *Nanomedicine (Lond)* 2(2): 219-232. doi: 10.2217/17435889.2.2.219
28. Heurtault B, Saulnier P, Pech B, Proust JE, Benoit JP. 2003. Physico-chemical stability of colloidal lipid particles. *Biomaterials* 24(23): 4283-4300. doi: 10.1016/S0142-9612(03)00331-4
29. Abdelwahed W, Degobert G, Stainmesse S, Fessi H. 2006. Freeze-drying of nanoparticles: formulation, process and storage considerations. *Adv Drug Deliv Rev* 58(15): 1688-1713. doi: 10.1016/j.addr.2006.09.017
30. Mainardes RM, Gremião MPD, Evangelista RC. 2006. Thermoanalytical study of praziquantel- loaded PLGA nanoparticles. *Rev Bras Ciências Farm* 42(4): 523-530. doi: 10.1590/S1516-93322006000400007
31. Surolia R, Pachauri M, Ghosh PC. 2012. Preparation and characterization of monensin loaded PLGA nanoparticles: *in vitro* anti-malarial activity against *Plasmodium falciparum*. *J Biomed Nanotechnol* 8(1): 172-181. doi: 10.1166/jbn.2012.1366
32. Feng SS, Mu L, Chen BH, Pack D. 2002. Polymeric nanospheres fabricated with natural emulsifiers for clinical administration of an anticancer drug paclitaxel (Taxol®). *Mater Sci Eng C* 20(1-2): 85-92. doi: 10.1016/S0928-4931(02)00017-6
33. Panyam J, Dali MM, Sahoo SK, Ma W, Chakravarthi SS, et al. 2003. Polymer degradation and *in vitro* release of a model protein from poly(D,L-lactide-co-glycolide) nano- and microparticles. *J Control Release* 92(1-2): 173-187. doi: 10.1016/S0168-3659(03)00328-6
34. Gonçalves C, Pereira P, Gama M. 2010. Self-assembled hydrogel nanoparticles for drug delivery applications. *Materials (Basel)* 3(2): 1420-1460. doi: 10.3390/ma3021420
35. Peppas LB. 1995. Recent advances on the use of biodegradable microparticles and nanoparticles in controlled drug-delivery. *Int J Pharm* 116(1): 1-9. doi: 10.1016/0378-5173(94)00324-X
36. Sturgeon RJ, Schulman SG. 1977. Electronic absorption spectra and protolytic equilibria of doxorubicin: Direct spectrophotometric determination of microconstants. *J Pharm Sci* 66(7): 958-961. doi: 10.1002/jps.2600660714
37. Keum CG, Noh YW, Baek JS, Lim JH, Hwang CJ, et al. 2011. Practical preparation procedures for docetaxel-loaded nanoparticles using polylactic acid-co-glycolic acid. *Int J Nanomedicine* 6: 2225-2234. doi: 10.2147/IJN.S24547
38. Chen Q, Xu R, Zeng C, Lu Q, Huang D, et al. 2014. Down-regulation of Gli transcription factor leads to the inhibition of migration and invasion of ovarian cancer cells via integrin β4- mediated FAK signaling. *PLoS One* 9(2): e88386. doi: 10.1371/journal.pone.0088386
39. Benvenuto M, Masuelli L, De Smaele E, Fantini M, Mattera R, et al. 2016. *In vitro* and *in vivo* inhibition of breast cancer cell growth by targeting the Hedgehog/GLI pathway with SMO (GDC-0449) or GLI (GANT-61) inhibitors. *Oncotarget* 7(8): 9250-9570. doi: 10.18632/oncotarget.7062
40. Bisht S, Feldmann G, Soni S, Ravi R, Karikar C, et al. 2007. Polymeric nanoparticle- encapsulated curcumin ("nanocurcumin"): a novel strategy for human cancer therapy. *J Nanobiotechnology* 5: 3. doi: 10.1186/1477-3155-5-3
41. Némati F, Dubernet C, de Verdière AC, Poupon MF, Treupel-Acar L, et al. 1994. Some parameters influencing cytotoxicity of free doxorubicin and doxorubicin-loaded nanoparticles in sensitive and multidrug resistant leucemic murine cells: incubation time, number of nanoparticles per cell. *Int J Pharm* 102(1-3): 55-62. doi: 10.1016/0378-5173(94)90039-6
42. Leroux J-C, Vargas A, Doelker E, Gurny R, Delie F. 2006. The use of drug-loaded nanoparticles in cancer chemotherapy. *Sect Title Pharm* 158: 625-671. doi: 10.1201/9781420027990.ch18
43. Cohen E, Ophir I, Shaul YB. 1999. Induced differentiation in HT29, a human colon adenocarcinoma cell line. *J Cell Sci* 112(Pt 16): 2657-2666.
44. Kenny PA, Lee GY, Myers CA, Neve RM, Semeiks JR, et al. 2007. The morphologies of breast cancer cell lines in three-dimensional assays correlate with their profiles of gene expression. *Mol Oncol* 1(1): 84-96. doi: 10.1016/j.molonc.2007.02.004
45. Onishi H. 2014. Hedgehog signaling pathway as a new therapeutic target in pancreatic cancer. *World J Gastroenterol* 20(9): 2335-2342. doi: 10.3748/wjg.v20.i9.2335
46. Al-Hajj M, Clarke MF. 2004. Self-renewal and solid tumor stem cells. *Oncogene* 23(43): 7274-7282. doi: 10.1038/sj.onc.1207947
47. Patel S, Rameshwar P. 2013. Tumorsphere passage for breast cancer stem cells. *Protoc Exch* 2013: 1-4. doi: 10.1038/protex.2013.023